CHEMISTRY
A EUROPEAN JOURNAL

DOI: 10.1002/chem.200701909

meso-Aryl Substituted Rubyrin and Its Higher Homologues: Structural Characterization and Chemical Properties

Soji Shimizu,[a] Won-Seob Cho,[b] Jonathan L. Sessler,*[b] Hiroshi Shinokubo,[a] and Atsuhiro Osuka*[a]

Abstract: *meso*-Aryl substituted rubyrin ([26]hexaphyrin(1.1.0.1.1.0)) **2** and a series of rubyrin-type large expanded porphyrins were obtained from a facile one-pot oxidative coupling reaction of *meso*-pentafluorophenyl substituted tripyrrane **1**. The structures of two of the resulting products were determined by single-crystal X-ray diffraction analysis. Whereas [52]dodecaphyrin(1.1.0.1.1.0.1.1.0.1.1.0) **4** takes a symmetric helical conformation, the larger species, [62]pentadecaphyrin(1.1.0.1.1.0.1.1.0.1.1.0.1.1.0) **5**, adopts a nonsymmetric distorted conformation in the solid state that contains an intramolecular helical structure. The ability of rubyrin **2** to act as an anion receptor in its diprotonated form (**2**·2H$^+$) was demonstrated in methanolic solutions. Oxidation of **2** with MnO_2 gave [24]rubyrin **6**, a species that displays antiaromatic characteristics. [26]Rubyrin **2** and [24]rubyrin **6** both underwent metallation when reacted with $Zn(OAc)_2$ to give the corresponding bis-zinc(II) complexes **7** and **8** quantitatively without engendering a change in the oxidation state of the ligands. As a result, complexes **7** and **8** exhibit aromatic and antiaromatic character, respectively. NICS calculation on these compounds also supported aromaticity of **2** and **7**, and antiaromaticity of **6** and **8**.

Keywords: anion recognition · aromaticity · conjugation · macrocyclic ligands · porphyrinoids

Introduction

Expanded porphyrins[1] are a relatively new class of functional molecules that have attracted considerable attention recently as selective anion receptors,[2] ligands for transition and lanthanoid ions,[3,4] photodynamic therapy photosensitizers,[5] and magnetic resonance imaging contrast agents.[6] Expanded porphyrins have also proved useful in the study of aromatic effects in large heterannulenes,[1] while, more recently, their large two-photon absorption cross sections, have made certain expanded porphyrins attractive for the study of three-dimensional micro-fabrication, optical data storage, and optical limiting effects.[7,8]

Many of the unique properties of fully conjugated expanded porphyrins, including whether they display aromatic features or display nonlinear optical effects, depend directly on the size of the macrocyclic ring.[1,7–18] Accordingly, one important research direction in expanded porphyrin chemistry has involved the preparation of ever larger systems. Unfortunately, the synthesis of such compounds remains challenging. Indeed, until recently, expanded porphyrins larger than octaphyrins were exceedingly rare.[15,19–21] Over the course of the last decade, the Kyoto group has developed a series of *meso*-aryl and *meso*-trifluoromethyl substituted expanded porphyrins, including a number that have demonstrated unique electronic properties and chemical reactivity.[17,21] Unfortunately, the synthetic strategies developed initially, involving the direct condensation of mono-pyrrole precursors with electron deficient aldehydes, are plagued by an inevitable drop in yield as the size of the macrocyclic products increases. Therefore, increasingly we have explored the use of preformed multi-pyrrole fragments. In the course of these investigations, specifically those targeting the synthesis of *meso*-pentafluorophenyl substituted rubyrin **2**[22,23] and [38]nonaphyrin(1.1.0.1.1.0.1.1.0) **3**,[24] we noticed that

[a] Dr. S. Shimizu, Prof. Dr. H. Shinokubo, Prof. Dr. A. Osuka
Department of Chemistry, Graduate School of Science
Kyoto University, Sakyo-ku, Kyoto 606-8502 (Japan)
Fax: (+81) 75-753-3970
E-mail: osuka@kuchem.kyoto-u.ac.jp

[b] Dr. W.-S. Cho, Prof. Dr. J. L. Sessler
Department of Chemistry and Biochemistry
1 University Station-A5300, The University of Texas at Austin
Austin, Texas 78712-0165 (USA)
Fax: (+1) 512-471-7550
E-mail: sessler@mail.utexas.edu

Supporting information for this article is available on the WWW under http://www.chemeurj.org/ or from the author.

oxidative coupling reaction involving tripyrrane **1** gave higher homologues in addition to **2** and **3**. We have now studied this condensation process in greater detail and wish to report here the successful isolation and characterization of [52]dodecaphyrin(1.1.0.1.1.0.1.1.0.1.1.0) **4** and [62]pentadecaphyrin(1.1.0.1.1.0.1.1.0.1.1.0.1.1.0) **5**. Pentadecaphyrin **5** is, to the best of our knowledge, the second largest expanded porphyrins structurally characterized to date.

In addition to reporting the isolation of expanded porphyrins **4** and **5**, we present further studies involving *meso*-pentafluorophenyl substituted rubyrin **2**. These involve analyses of its anion binding behavior of the diprotonated form and oxidation/metallation studies of the neutral macrocycle, respectively. The first of these studies was motivated by the finding in initial work that diprotonated rubyrin, $\mathbf{2}\cdot 2H^+$, exhibited two different conformations depending on the choice of counter anions.[23] Such an observation, which is thought to reflect the greater flexibility of *meso*-substituted rubyrins around the pyrrole–pyrrole linkage than the corresponding *meso*-free, β-alkyl functionalized derivatives,[22a] thus provided a specific incentive to examine the anion binding properties of $\mathbf{2}\cdot 2H^+$ in detail. Surprisingly, this is something that has not been in the case of *meso*-functionalized (as opposed to β-alkyl substituted) expanded poprhyrins.

The second set of studies was motivated by recent findings that certain hexapyrrolic expanded porphyrins undergo conversion from the corresponding aromatic to antiaromatic forms (or vice versa) upon metallation.[7b,25,26] Such "switching", which gives rise to easy-to-assess changes in electronic and optical properties, is noteworthy given the normal difficulties associated with isolating planar structures with Hückel-type antiaromatic conjugation.[25,26] It was thus of interest to see if rubyrin **2**, a 26 π-electron species, could be oxidized to the corresponding 24 π-electron antiaromatic species and whether prior or concurrent metallation was required to effect the transformation. As detailed below, *meso*-pentafluorophenyl substituted rubyrin **2** can indeed be oxidized to its antiaromatic derivative, [24]rubyrin **6**, by treatment with MnO_2. As such, system **2** stands a further rare example of a switchable aromatic–antiaromatic molecule.

Results and Discussion

Synthesis of *meso*-pentafluorophenyl substituted rubyrin and its higher homologues: In the course of our studies on expanded porphyrins, we noted the benefit of the electron-deficient pentafluorophenyl group for the formation of *meso*-aryl substituted expanded porphyrins from the acid catalyzed reaction between aromatic aldehydes and simple pyrroles.[17] Although the role of this and related deactivating groups remains to be elucidated fully, one plausible explanation is that such substituents stabilize the porphyrinogen precursors, presumed to be formed during the course of reaction, against possible scrambling under acidic conditions. In light of such considerations, we examined the oxidative coupling reaction of *meso*-pentafluorophenyl substituted tripyrrane **1** under conditions similar to those used in the synthesis of core-modified rubyrins by Chandrashekar et al. (TFA, CH_2Cl_2, followed by chloranil).[22] After work up, the resulting reaction mixture was separated over a neutral alumina column to give two fractions. The second violet fraction proved to be rubyrin ([26]hexaphyrin(1.1.0.1.1.0)) **2**, a product that was further purified by chromatography over silica gel to give a pure sample in 24% yield.[23] The first fraction was subject to further separation using size exclusion chromatography; this provided the previously characterized species [38]nonaphyrin(1.1.0.1.1.0.1.1.0) **3** in 9% yield,[23] as well as the new products [52]dodecaphyrin-(1.1.0.1.1.0.1.1.0.1.1.0) **4** and [62]pentadecaphyrin-(1.1.0.1.1.0.1.1.0.1.1.0.1.1.0) **5** in isolated yields of 2.7 and 1.5%, respectively (Scheme 1). The isolated yields of **4** and **5**, while modest, proved fully reproducible.

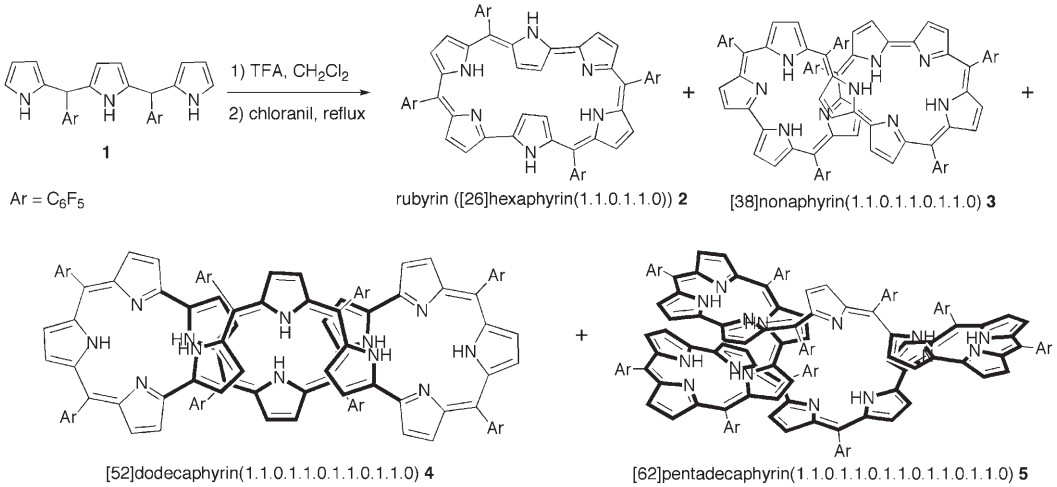

Scheme 1. Synthesis of rubyrin and its higher homologues.

Spectroscopic and structural characterization of [52]dodecaphyrin(1.1.0.1.1.0.1.1.0.1.1.0) and [62]pentadecaphyrin-(1.1.0.1.1.0.1.1.0.1.1.0.1.1.0): High-resolution electrospray-ionization time-of-flight (HR-ESI-TOF) mass spectrometry revealed an ion peak at *m*/*z* 2207.2089, a finding consistent with **4** being a dodecapyrrolic macrocycle (calcd for a parent [M^-−H] peak, $C_{104}N_{12}F_{40}H_{31}$, 2207.2161). The absorption spectrum showed rather featureless broad bands at 327, 412, 657, and 784 nm (Figure 1). The ^{1}H NMR spectrum of **4** was characterized by a very simple pattern of signals at δ 7.18, 7.05, 6.78, 6.71, 6.35, and 6.19 ppm, ascribable to the β-CH protons, and resonances at δ 14.40, 8.66, and 7.23 ppm due to the NH protons, as would be anticipated for a highly symmetric conformation (see Supporting Information). This assignment was also supported by the clean nature of the ^{19}F NMR spectrum recorded for **4**.

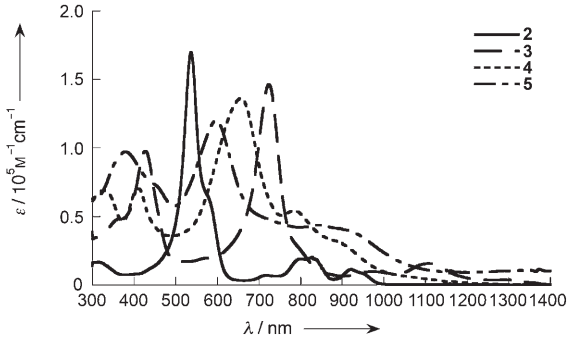

Figure 1. UV/Vis absorption spectra of rubyrin and its higher homologues recorded in CH_2Cl_2.

Single crystals of **4** were obtained via the vapor diffusion of hexane into a CH_2Cl_2 solution. X-ray diffraction analysis of **4** revealed a near D_{2h} symmetric twisted structure consisting of two inward-orienting tripyrrane units (pyrroles L, A, and B, and F, G, and H) and two tripyrrane units with two inverted pyrrole rings (pyrroles C, D, and E, and I, J, and K) (Figure 2). Intramolecular hydrogen bonding interactions were observed between adjacent sets of amine-like pyrrole NH protons and neighboring unprotonated imine-like nitrogen atoms (N-H···N distances and angles; 2.10 Å and 123.8° (pyrroles A and B), 2.21 Å and 122.9° (pyrroles F and G), 2.10 Å and 123.8° (pyrrole G and H), and 2.21 Å and 122.1° (pyrroles L and A)). Presumably, these multiple hydrogen-bonding interactions serve to maintain the conformation seen in the solid state and help account for the rigid structure observed in solution, as inferred from the NMR spectral data alluded to above.

The HR-ESI-TOF mass spectrum of **5** revealed a parent ion peak at *m*/*z* 2756.2530 ([M^-−H]; calcd for $C_{130}N_{15}F_{50}H_{36}$ 2756.2485) corresponding to the proposed structure. The absorption spectrum exhibited relatively sharp bands at 379 and 598 nm, along with a broad absorption tail that reaches into the near-IR region (Figure 1). The ^{1}H NMR spectrum of **5** was too broad to assign at room temperature and remained broad upon cooling at −20 °C, displaying signals in a range of 4–8 ppm. The ^{19}F NMR spectrum of **5** at −20 °C in $CDCl_3$ was still broad, but was sufficiently well resolved to allow for assignment (see Supporting Information). In particular, the integrations are consistent with the number of fluorine atoms at the various positions (e.g., twenty fluorine atoms for the *ortho* and *meta* positions and ten atoms for the *para* substituents). These spectral features can be understood in terms of compound **5** being non-rigid in solution and subject to considerable conformational flexibility under conditions of the ^{1}H and ^{19}F NMR spectroscopic analyses.

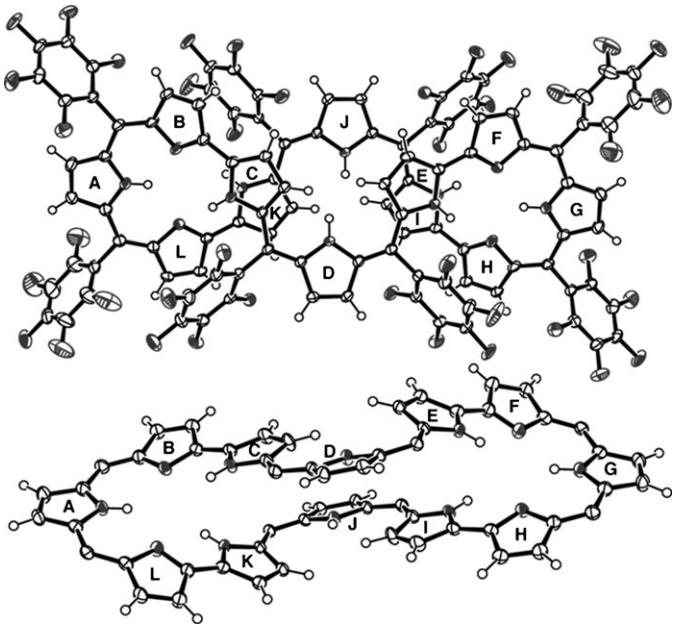

Figure 2. X-ray crystal structure of **4**, top view (top) and side view (below). The thermal ellipsoids are scaled to the 50% probability level. The pentafluorophenyl substituents at the *meso*-positions are omitted for clarity in the side view.

Macrocycle **5** was characterized more fully by single crystal X-ray diffraction analysis; the resulting structure revealed the system to be nonsymmetric with a helically wound moiety (Figure 3). Intramolecular hydrogen bonding networks between the amine NH and the imine N of pyrrole rings in **5** presumably serve to stabilize this helical conformation (N-H···N distances and angles; 2.18 Å and 122.2° (pyrroles A and B), 2.15 Å and 122.0° (pyrroles B and C), 2.17 Å and 120.4° (pyrroles G and H), 2.15 Å and 122.5° (pyrroles H and I), 2.29 Å and 122.1° (pyrroles J and K), 2.08 Å and 124.7° (pyrroles K and L), and 2.01 Å and 127.3° (pyrroles N and O)). As can be seen from inspection of Figure 3, the thermal ellipsoids of the smaller helical moiety from the pyrrole A to the pyrrole D are larger than the others. This proved true even though the data set was recorded at low temperature (−183 °C). Moreover, several sets of crystals of **5** were subject to structural analyses. In all cases, the thermal ellipsoids were always comparatively large at this moiety, and in some instances this part proved highly disordered. These findings are thought to reflect the

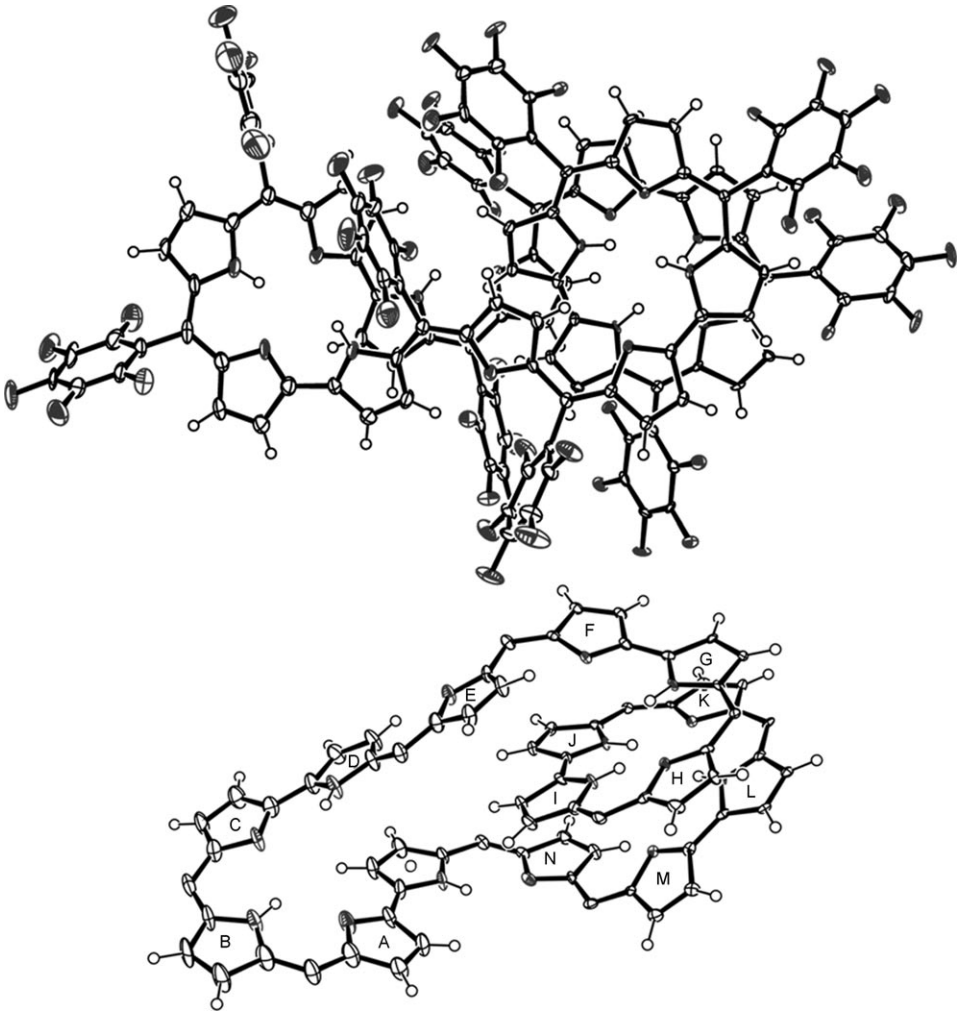

Figure 3. X-ray crystal structure of **5**, top view (top) and side view (below). The thermal ellipsoids are scaled to the 50% probability level. The pentafluorophenyl substituents at the *meso*-positions are omitted for clarity in the side view.

conformational flexibility observed in solution, and thus help account for the broad signals observed in the solution phase ^{1}H and ^{19}F NMR spectra.

Anion recognition behavior of protonated rubyrin: As previously reported, rubyrin **2** can take three different conformations (type I, II, and III) depending upon its protonation state (see below).[23] Whereas the free base rubyrin **2** adopts a conformation of type I, the conformation of the diprotonated species was found to depend on the choice of acid; a type II conformation is preferred upon protonation with trifluoroacetic acid, whereas a type III conformation is preferred upon protonation with HCl. These structural changes were fully characterized by NMR and X-ray analyses. Due to changes in the conjugation pathway, these two protonated forms exhibit different Soret-like absorptions, namely at 555 nm for type II and at 518 nm for type III (cf. Supporting Information).

We have now extended our protonation studies to include H_2SO_4 and H_3PO_4. Both of these acids give rise to protonated forms of **2** (i.e., **2**·2H$^+$) characterized by split Soret-like bands at 520 and 550 nm that, on the basis of the above findings, are interpreted in terms of the presence of both type II and III conformations. To the extent such an interpretation is correct, it indicates that the choice of counter anion can have a large effect on the conformation of **2**·2H$^+$. This, in turn, prompted us to investigate the anion recognition behavior of **2**·2H$^+$ in greater detail. Towards this end, hydriodic acid was chosen as a proton source with the expectation that the counter iodide anion would be weakly bound to **2**·2H$^+$ and hence easily exchanged by other anions.[27] Thus, hydriodic acid was added to a about 4.0×10^{-3} mM solution of rubyrin **2** while the changes in the UV/Vis absorption spectrum were recorded. After the addition of $\geq$25 molar equivalents, no further spectral changes were seen, leading to the inference that full conversion to the diprotonated form **2**·2H$^+$

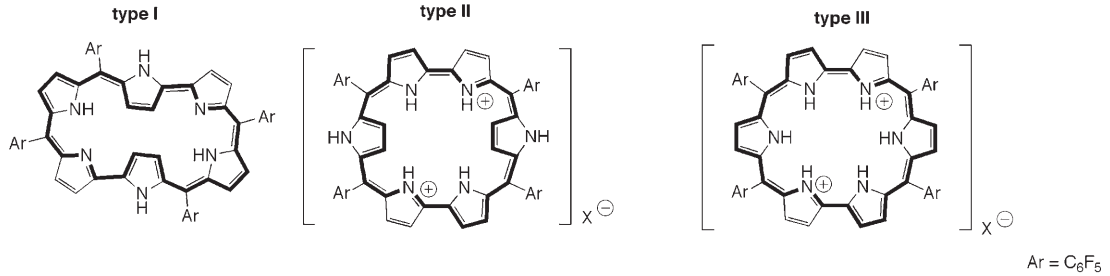

had been effected (see Supporting Information). The final spectrum obtained in this way is characterized by a Soret-like band at about 550 nm, from which it is inferred that **2**·2H$^+$ exists in a type II conformation. The methanolic solution of **2**·2H$^+$ produced in this way was then subject to titration with either chloride (0–2.0 equiv) or sulfate (0–4.3 equiv) anions (studied as their corresponding tetrabutylammonium and tetramethylammonium salts, respectively) and again the spectral changes were recorded (cf. Figure 4).

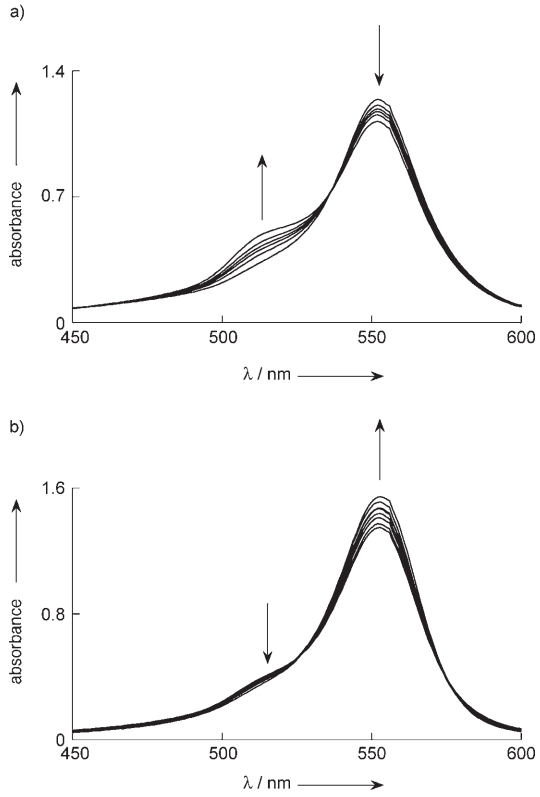

Figure 4. UV/Vis absorption spectral changes of protonated rubyrin **2** (**2**·2H$^+$) (4.0×10^{-3} mM methanolic solution as produced by pretreatment with 25 equiv of hydriodic acid) observed upon the addition of a) tetrabutylammonium chloride (0–2.0 equiv of Cl^-) and b) tetramethylammonium sulfate (0–4.3 equiv of SO_4^{2-}).

Addition of chloride anion resulted in a decrease in the absorbance intensity at 552 nm and an increase in that at 513 nm. On the basis of the prior analyses (see above), such a result is considered consistent with a change in conformation from type II to type III as the result of chloride-for-iodide anion exchange (Figure 4a). In contrast, the addition of sulfate anion led to a decrease in the intensity of the shoulder-like absorption at 513 nm and an increase in the intensity of the absorbance at 552 nm (Figure 4b). This result, which stands in contrast to the formation of two protonated conformers upon simple protonation of **2** with sulfuric acid, is of particular interest, since it indicates that the pre-organization of type II conformation has a large influence on the anion recognition properties. In fact, we interpret the titration experiment (Figure 4b) with sulfate anion in terms of anion exchange of iodide anion by sulfate anion, which causes rigidification of a type II conformation. In both titration experiments, standard curve fits matched well with a 1:1 binding profile (cf. Supporting Information), which was also supported by Job-plot analyses. Given this, apparent binding constants on the order of $10^4\,M^{-1}$ and $10^5\,M^{-1}$ for chloride anion and sulfate anion, respectively, could be estimated from the absorption changes at 513 nm and at 552 nm, respectively. However, it is important to appreciate that these values represent formal exchange constants (unitless) and can be taken as apparent affinity constants only to the extent the limiting assumption that the initial iodide anion is not bound is valid. Further, as with many analyses of this type, the actual values were found to be rather sensitive to the extent to which the anion salt in question, the methanol solvent, and the rubyrin itself were rigorously dried.

Oxidation of [26]rubyrin to antiaromatic [24]rubyrin: An attractive feature of nitrogen-containing porphyrins and expanded porphyrins is the ability to adopt two-electron oxidation and reduction reactions through facile release and uptake of two hydrogen atoms on the nitrogen atoms; in principle, this allows for the existence of neutral forms for multiple oxidation states.[14,17,21,25,28] A two-electron redox process is expected to induce a sharp Hückel type aromatic-to-antiaromatic switch when the macrocyclic framework is maintained, as recently demonstrated for bis-gold(III) hexaphyrin(1.1.1.1.1.1) complexes[25b,c] and a uranyl hexaphyrin(0.0.0.0.0.0) complex.[26c] However, we are unaware of any fully characterized system of expanded porphyrins where this has been demonstrated in the absence of metallation except for *meso*-pentafluorophenyl substituted N-fused [24]pentaphyrin[25a] and tetrathiaoctaphyrins.[14] However their paratropic ring current effect were found to be subtle presumably because of their highly distorted structures. We thus keen to determine if such a conversion could be carried out in the case of rubyrin **2** ([26]hexaphyrin(1.1.0.1.1.0)). This species was thus treated with DDQ. Although this did indeed provide a new spot on the thin layer chromatogram, we could not purify the resulting putative new compound through silica gel or alumina column. While not fully established, the problem appeared to be that under both sets of chromatographic conditions facile reduction back to **2** occurs. Therefore, **2** was subject to oxidation with MnO_2. The use of this inorganic oxidant simplified purification, in that after the reaction, the residual inorganic solids were simply removed by filtration to give the oxidized form of **2**, the [24]rubyrin **6**, in almost quantitative yield. Compound **6** can be easily reduced back to **2** upon treatment with $NaBH_4$.

The formally antiaromatic species **6** was fully characterized by spectroscopic means. Consistent with the proposed structure, the ^{1}H NMR spectrum of **6** recorded in $CDCl_3$ solution revealed resonances for the inner β-CH protons as a pair of doublet ($J=4.8$ Hz) at δ 12.57 and 11.80 ppm, respectively. Signals ascribable to the outer β-CH protons

were seen at δ 5.82, 5.66, 5.41, and 5.18 ppm; these appeared as two pairs of mutually coupled signals ($J = 4.6$ Hz) (Figure 5). An extremely down-field shifted signal at δ 21.77 ppm was assigned to the inner NH protons. HH-COSY spectrum of **6** revealed correlation between the peaks at δ 12.57 and 11.80 ppm, 5.82 and 5.66 ppm, and 5.41 and 5.18 ppm, respectively. Further structural information was provided by ROESY measurement, which reveals proximity of spatially neighboring protons (see Supporting Information). In the ROESY spectrum of **6**, the correlation between the inner NH proton and the outward orienting pyrrole proton at 12.57 ppm was observed. In addition, in-depth inspection of the ^{1}H NMR spectrum of **6** reveals double-doublet splitting of the peak at 5.18 ppm, which is accounted for the long range proton-proton coupling between NH and the outer β-CH. Overall, these findings are consistent with the oxidized species **6** possessing a rectangular conformation similar to that of **2** in solution, as well as displaying a distinctive paratropic ring current, which presumably arises from its 24 π-electron conjugation pathway.[25,26] The UV/Vis spectrum of **6** recorded in dichloromethane solution exhibited a blue-shift in the less intense Soret-like band (relative to **2**) but no appreciable low-energy Q-band like band. Such spectral features mirror those seen for the antiaromatic gold complexes of the [28]hexaphyrins (Figure 6).[25b] Unfortunately, while compound **6** proved stable under typical laboratory conditions, all efforts to obtain single crystals of this species that would be suitable for X-ray analysis were stymied due to its poor solubility and lack of long-term stability.

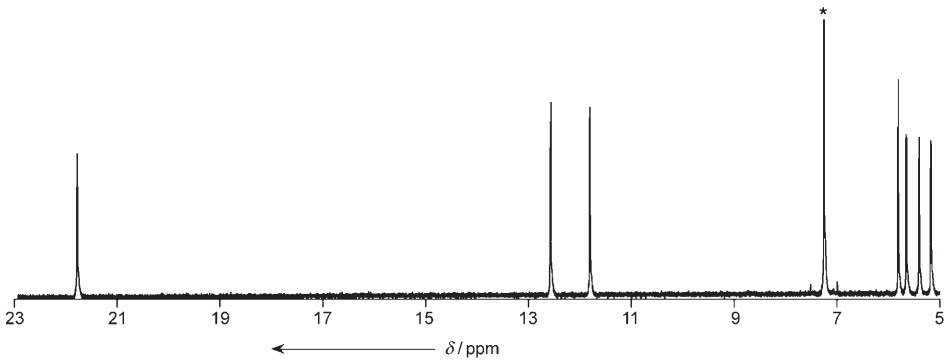

Figure 5. ^{1}H NMR spectrum of **6** recorded in $CDCl_3$.

Zinc metallations of 2 and 6: Given the fact that aromatic and antiaromatic forms had been characterized previously for several other hexapyrrolic expanded porphyrins (see above), it was of interest to us to see if metallation of the two rubyrins **2** and **6** would lead to changes in oxidation state. Such a study is made more compelling by the fact that these two species differ from one another only in terms of the number of π-electrons within their respective conjugation pathways and the charges of the fully deprotonated forms as a direct consequence of the differing number of NH protons. Zinc(II) was chosen for these studies because it is diamagnetic and would permit the proposed metal insertion reactions to be followed by NMR spectroscopy.

Initially, metallation of **2** with $Zn(OAc)_2$ was attempted in a mixture of CH_2Cl_2 and methanol with zinc acetate. The metallation proceeded smoothly with the color of the solution changing from violet to bright red, a transformation that was ascribed to quantitative conversion to the bis-zinc complex **7** (see below). After the metallation was complete, the solvent was removed using a rotary evaporator. The residue was then dissolved in a small amount of CH_2Cl_2, upon which hexane was layered to induce precipitation of the inorganic salts. These latter were then removed by filtration. A preliminary single crystal X-ray diffraction analysis was performed; the resulting structure revealed a bis-zinc complex possessing a type III conformation, in which the two cations are bound by two dipyrromethene subunits, while the two remaining pyrrolic units do not interact with the zinc ions (see Supporting Information). The two zinc ions are bridged by an acetate anion as well as by an oxygen atom of a hydroxy group. Consistent with the formulation of **7** as a complex of [26]rubyrin, the ^{1}H NMR spectrum of **7** clearly indi-

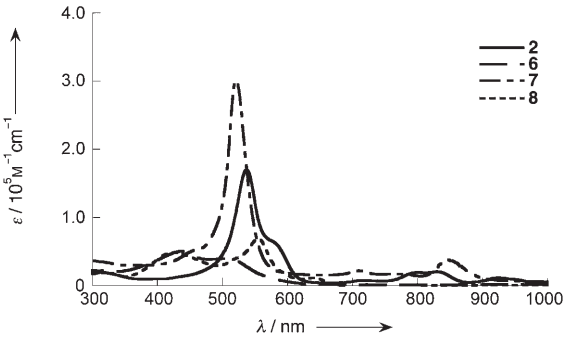

Figure 6. UV/Vis absorption spectra of rubyrin **2**, [24]rubyrin **6**, and their respective bis-zinc complexes **7** and **8** as recorded in CH_2Cl_2.

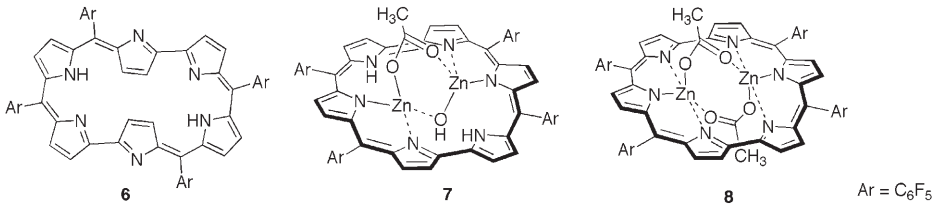

cated a strong diatropic ring current. This was evidenced by signals for those protons held within the center of the ring, namely those for the acetate, hydroxy, and the uncomplexed pyrrolic NH group, at δ −2.87, −8.97, and −5.14 ppm, respectively, being positioned in a shielded region. Conversely, the signals ascribable to the outer β-CH protons were observed in a deshielded region at δ 10.88, 10.37, 9.57, 9.52, 9.34, and 9.04 ppm.

The bis-zinc complex of the oxidized [24]rubyrin **6** was synthesized and purified in a similar way. The absorption spectrum of the resulting bis-zinc complex, **8**, is characterized by an ill-defined broad absorption without any Q-like absorption (Figure 6). Moreover, its ^{1}H NMR spectrum shows three peaks due to the β-CH protons at δ 6.16, 5.22, and 5.15 ppm, as well a peak at 4.02 ppm assigned to the methyl groups of the two bound acetate anions. Thus, even though the species were produced by independent synthesis, the chemical shifts of the methyl group of the bridging acetate was "shifted" from −2.87 ppm in **7** to 4.02 ppm in **8**, a finding that is fully consistent with the large proposed differences in the electronics of these two systems.

The structure of **8** was elucidated by single crystal X-ray analysis, and was found to possess a type III conformation. Thus, the two zinc ions coordinated by this antiaromatic rubyrin were found to be bridged by an acetate group, as well as by a single oxygen atom arising from the other acetate counter anion (Figure 7). Although the non-identical nature of the acetate bridging seen in the solid state is slightly different from what might be inferred from the symmetrical structure one would infer from the ^{1}H NMR spectrum, the difference can easily be accounted for in terms of "normal" variations, such as crystal packing or, more likely, fast exchange on the ^{1}H NMR time scale. In any event, apart such small differences, it is important to appreciate that the structure of **8** is consistent with its formulation as a 24π-electron expanded porphyrin. For instance, the side view of this complex reveals the highly distorted nature of the structure. Nonetheless, in spite of its nonplanar nature, the ^{1}H NMR spectrum of the bis-zinc complex of this antiaromatic [24]rubyrin exhibits a slight up-field shift for the outer β-CH proton resonances and a down-field shift of the inner acetate protons due to the presumed presence of a paratropic ring current effect. Taken in concert, such findings provide support for the notion that both rubyrins **2** and **6** undergo zinc(II) metallation without a change in their respective oxidation states; thus the number of π-electrons in the bis-zinc(II) complexes **7** and **8** are the same as those present in **2** and **6**, respectively. On this basis, they are characterized aromatic and antiaromatic, respectively.

Quantitative analyses of aromaticity and antiaromaticity of compounds 2, 6, 7, and 8: To evaluate aromaticity and antiaromaticity of rubyrins **2**, **6**, **7**, and **8**, we have carried out theoretical calculations by the DFT (B3LYP/6-31G* (LANL2DZ for Zn)) method[29,30] on the model compounds where pentafluorophenyl substituents of the real systems were replaced with protons for simplicity. Nucleus-independent chemical shifts (NICS)[31] were obtained as the qualitative measure for aromaticity and antiaromaticity on optimized structures. The NICS values were calculated on the global ring center of macrocycles, as well as centers of each pyrrole unit and formal ring structure between two adjacent pyrroles, as shown in Figure 8. Clearly, [26]rubyrin **2** is strongly aromatic, for which the NICS value was calculated to be −18.2 ppm at the center of the molecule. On the other hand, [24]rubyrin **6** exhibits a moderately positive NICS value (+6.5 ppm) at the center. Moreover, NICS values at the points 3, 5, 7, 9, 11, and 13 are substantially large positive (11.3–16.1 ppm, Table 1). On the basis of these results, we conclude that [24]rubyrin **6** has substantial antiaromaticity, which is also experimentally indicated by the ^{1}H NMR and absorption spectra.

For bis-zinc complexes of rubyrins, NICS values of **7** and **8** at the ring centers are −25.4 and +9.2 ppm, respectively, suggesting **7** to be aromatic and **8** to be antiaromatic. This indication is also in good agreement with experimental data.

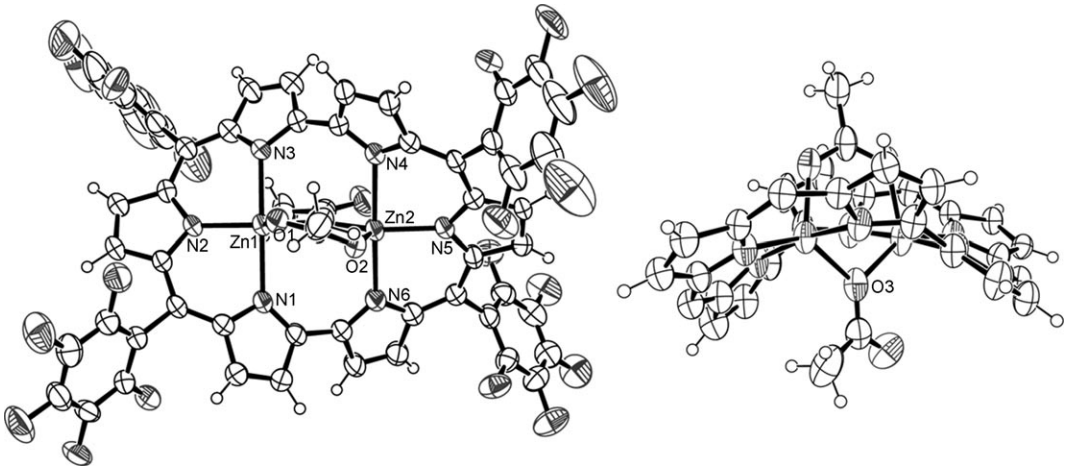

Figure 7. X-ray crystal structure of **8**, top view (left) and side view (right). The thermal ellipsoids are scaled to the 50% probability level. The pentafluorophenyl substituents at the *meso*-positions are omitted for clarity in the side view.

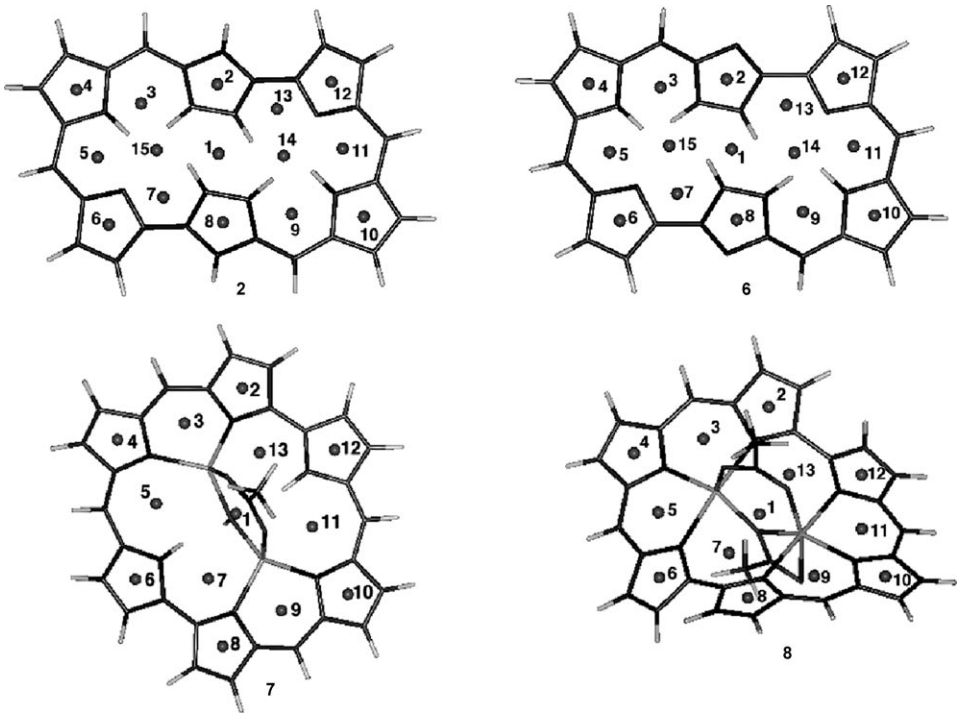

Figure 8. Optimized structures of models for compounds **2**, **6**, **7**, and **8**. Points for the NICS calculations are also shown.

Table 1. NICS values [ppm] of the selected points as depicted in Figure 8.

Point	**2**	**6**	**7**	**8**
1	−18.2	6.5	−25.4	9.2
2	−12.4	6.5	−10.8	−1.6
3	−19.5	11.3	−22.6	23.4
4	−13.4	−5.9	−10.9	−3.7
5	−17.1	16.1	−20.4	23.0
6	−3.5	−5.2	−17.4	−1.5
7	−18.1	12.1	−20.8	18.8
8	−12.4	6.5	−10.8	−2.4
9	−18.8	11.3	−22.6	23.3
10	−13.4	−5.9	−10.9	−4.6
11	−17.1	16.1	−20.4	23.5
12	−3.5	−5.2	−17.4	−2.2
13	−18.1	12.1	−20.8	19.0
14	−15.4	9.7		
15	−15.4	9.7		

Again, NICS values of **8** at centers of formal ring structures between two adjacent pyrroles (point 3, 5, 7, 9, 11, and 13) are significantly large positive (18.8–23.5 ppm).

Conclusion

The coupling reaction of tripyrrane **1** with TFA and chloranil provide large expanded porphyrins **4** and **5** in addition to **2** and **3**. [62]Pentadecaphyrin(1.1.0.1.1.0.1.1.0.1.1.0.1.1.0) **5** is the second largest expanded porphyrins structurally characterized so far. The protonated form of rubyrin rubyrin **2** acts as an effective anion receptor for the chloride and sulfate anions, as revealed by anion exchange experiments monitored by UV/Vis spectroscopy. [26]Rubyrin **2** exhibits a diatropic ring current, as would be expected given its 26 π-electron aromatic nature. In contrast, its two-electron oxidized form, [24]rubyrin **6**, prepared by the oxidation of **2** with MnO_2, displays a paratropic ring current consistent with an antiaromatic character. Both **2** and **6** are metallated readily with zinc(II) ions to provide the corresponding bis-zinc complexes **7** and **8** in quantitative yields. Both sets of complexes adopt type III conformations with all the pyrrole rings pointing inward. They both retain the fundamental conjugation pathways present in the initial non-metallated species (i.e., ligands **2** and **6**). They thus display diatropic and paratropic ring currents, respectively, which are also supported by quantitative analyses of the optimized structures by using NICS values. The unique properties displayed by these rubyrins make both of them and their larger congeners, including **3**, **4** and **5**, attractive systems with which to study the effects of both cation coordination and anion binding on conformational motion and aromatic–antiaromatic switching. Further studies of these and related systems are thus ongoing in our laboratories.

Experimental Section

General procedure: All reagents and solvents were of commercial reagent grade and were used without further purification except where noted. Dry CH_2Cl_2 was obtained by distilling over CaH_2. ^1H and ^{19}F NMR spectra were recorded on a JEOL ECA-600 spectrometer (operating as 600.17 MHz for ^1H and 564.73 MHz for ^{19}F) using the residual solvent as the internal reference for ^1H ($\delta = 7.260$ ppm for $CDCl_3$) and hexafluorobenzene as an external reference for ^{19}F ($\delta = -162.9$ ppm). Spectroscopic grade CH_2Cl_2 was used as the solvent for all spectroscopic studies, except those involving anion binding, which were carried out in methanol. UV-visible absorption spectra were recorded on a Shimadzu UV-3100 spectrometer. Mass spectra were recorded on a JEOL HX-110 spectrometer using the positive-FAB ionization method with an accelerating voltage 10 kV and a 3-nitrobenzylalcohol matrix, or on a Shimadzu/KRATOS KOMPACT MALDI 4 spectrometer using the positive-MALDI ionization method. ESI-TOF-MS spectra were recorded on a BRUKER microTOF, using either the positive and negative-ion modes; acetonitrile was used as the solvent. Preparative separations were performed by silica gel flash column chromatography (Merck Kieselgel 60H Art. 7736), silica gel gravity column chromatography (Wako gel C-400),

or recycling preparative GPC-HPLC (JAI LC-908 with preparative JAIGEL-2H, 2.5H, and 3H columns).

Crystallographic data collection and structure refinement: Data collection for compound **8** was carried out at low temperature (−153 °C) on a Rigaku RAXIS-RAPID with graphite monochromated $Mo_{K\alpha}$ radiation ($\lambda = 0.71069$ Å), whereas data for **4** and **5** was collected at −183 °C on a Bruker SMART APEX with graphite monochromated $Mo_{K\alpha}$ radiation ($\lambda = 0.71069$ Å). Details of the crystallographic data are listed in Table 2.

Table 2. Crystallographic details for **4**, **5**, and **8**.

	4	**5**	**8**
empirical formula	$C_{104}N_{12}F_{40}H_{36}Cl_{12}$	$C_{137}N_{15}F_{50}H_{53}$	$C_{56}N_6F_{20}H_{18}O_4Zn_2$
M_r	2710.91	2858.94	1349.50
crystal system	triclinic	monoclinic	monoclinic
space group	$P\bar{1}$ (2)	$P2_1/c$ (14)	$P2_1/a$ (14)
a [Å]	9.7166(15)	36.091(3)	13.851(3)
b [Å]	15.142(2)	24.210(2)	23.024(5)
c [Å]	18.476(3)	15.1930(14)	17.798(4)
α [°]	84.703(2)	90	90
β [°]	75.046(2)	99.043(2)	106.429(7)
γ [°]	89.022(2)	90	90
V [Å^3]	2614.9(7)	13110(2)	5444(2)
Z	1	4	4
ρ [g cm^{-3}]	1.722	1.448	1.646
μ [mm^{-1}]	0.448 ($Mo_{K\alpha}$)	0.137 ($Mo_{K\alpha}$)	1.003 ($Mo_{K\alpha}$)
F(000)	1344	5720	2672
crystal size [mm^3]	0.80x0.40x0.20	0.30x0.30x0.10	0.25x0.25x0.10
$2\theta_{max}$ [°]	50.0	50.0	55.0
T [K]	90(2)	90(2)	123(2)
diffractometer	Smart Apex	Smart Apex	Raxis Rapid
total reflections	24893	66886	52391
unique reflections	9162	22974	12390
reflection used	9162	22974	12390
parameters	822	1822	795
absorption correction	empirical	empirical	none
R_1	0.0958	0.1031	0.0781
wR_2	0.2985	0.2357	0.2248
GOF	1.048	1.129	1.050

The structures were solved by direct methods (Sir 97[32] or SHELXS-97[33]) using the full-matrix least square technique (SHELXL-97).[33] Solvent molecules contained in the lattice of **8** were severely disordered and could not be resolved. The program SQUEEZE[34a] in PLATON[34b] was used to remove the solvent electron density.

CCDC 658457 (**4**), 658458 (**5**) and 658459 (**8**) contain the supplementary crystallographic data for this paper. These data can be obtained free of charge from The Cambridge Crystallographic Data Centre via www.ccdc.cam.ac.uk/data_request/cif.

Synthesis of rubyrin 2 and higher homologues: TFA (30.6 μL, 0.4 mmol) was added to a solution of **1** (450 mg, 0.81 mmol) in CH_2Cl_2 (90 mL). The resulting solution was stirred for 90 min at room temperature under a nitrogen atmosphere. At this point, chloranil (594 mg, 2.63 mmol) was added and the mixture was heated at reflux for a further 90 min. The reaction was quenched by the addition of aqueous $NaHCO_3$, and the organic layer was washed once with water, and dried over anhydrous Na_2SO_4. After removal of solvent, the crude product was purified over a neutral alumina column using a mixture of CH_2Cl_2/hexane as an eluent. After elution of deeply colored fractions, a purple fraction was eluted with CH_2Cl_2, which gave **2** (107 mg, 24 %). The first eluted fraction from this alumina column was further purified by gel-permeation chromatography to give **3**, **4**, and **5** in yields of 9.0, 2.7, and 1.5 %, respectively.

***meso*-Pentafluorophenyl substituted [52]dodecaphyrin(1.1.0.1.1.0.1.1.0.1.1.0) 4**: ^{1}H NMR (600 MHz, $CDCl_3$, 298 K): $\delta = 14.40$ (brs, 2H; NH), 8.66 (brs, 4H; NH), 7.23 (brs, 2H; NH), 7.18 (brs, 4H; β-CH), 7.05 (brs, 4H; β-CH), 6.78 (d, $J = 4.6$ Hz, 4H; β-CH), 6.71 (d, $J = 4.0$ Hz, 4H; β-CH), 6.35 (brs, 4H; β-CH), 6.19 ppm (s, 4H; β-CH); ^{19}F NMR (565 MHz, $CDCl_3$, 298 K): $\delta = -136.3$ (d, $J = 24.1$ Hz, 4F; *o*-F), −136.4 (d, $J = 20.7$ Hz, 4F; *o*-F), −139.5 (dd, $J = 23.3$ Hz, $J = 7.7$ Hz; 4F; *o*-F), −140.0 (brs, 4F; *o*-F), −153.4 (t, $J = 20.7$ Hz, 4F; *p*-F) −153.6 (q, $J = 20.7$ Hz, 4F; *p*-F), −158.2 (m, 4F; *m*-F), −160.2 (brs, 4F; *m*-F), −161.8 (m, 4F; *m*-F), −162.0 ppm (m, 4F; *m*-F); UV/Vis (CH_2Cl_2): λ_{max} (ε) = 327 (69000), 412 (70000), 657 (136000), 784 nm (54000 M^{-1} cm^{-1}); HR-ESI-TOF-MS: *m*/*z* (%): calcd for $C_{104}N_{12}F_{40}H_{31}$: 2207.2161; found: 2207.2089 (100) [M^-−H].

***meso*-Pentafluorophenyl substituted [62]pentadecaphyrin(1.1.0.1.1.0.1.1.0.1.1.0.1.1.0) 5**: ^{19}F NMR (565 MHz, $CDCl_3$, 253 K): $\delta =$ −134.5 (brs, 1F; *o*-F), −136.0–−137.19 (broad peaks, 12F; *o*-F), −138.0 (brs, 1F; *o*-F), −139.2 (brs, 1F; *o*-F), −139.3 (d, $J = 21.5$ Hz, 1F; *o*-F), −139.5 (d, $J = 22.6$ Hz, 1F; *o*-F), −140.9 (brs, 1F; *o*-F), −141.3 (brs, 1F; *o*-F), −141.5 (brs, 1F; *o*-F), −151.8 (brs, 1F; *p*-F), −152.1 (brs, 2F; *p*-F), −152.5 (brs, 1F; *p*-F), −152.5–−153.1 (broad peaks, 3F; *p*-F), −154.0 (brs, 1F; *p*-F), −154.2 (brs, 1F; *p*-F), −154.8 (brs, 1F; *p*-F), −159.6 (brs, 1F; *m*-F), −160.6 (m, 2F; *m*-F), −160.8 (brs, 1F; *m*-F), −161.3–−161.4 (broad peaks, 3F; *m*-F), −161.6 (brs, 2F; *m*-F), −162.2 (m, 1F; *m*-F), −162.5 (m, 1F; *m*-F), −162.6 (m, 1F; *m*-F), −163.0–−163.1 (m, 2F; *m*-F), −163.4 (brs, 1F; *m*-F), −164.1 (brs, 1F; *m*-F), −164.4–−164.5 (m, 3F; *m*-F), −165.4 ppm (brs, 1F; *m*-F); UV/Vis (CH_2Cl_2): λ_{max} (ε) = 379 (97000), 598 nm (120000 M^{-1} cm^{-1}); HR-ESI-TOF-MS: *m*/*z* (%): calcd for $C_{130}N_{15}F_{50}H_{36}$: 2756.2485; found: 2756.2530 (100) [M^-−H].

[24]Rubyrin 6: An excess amount of MnO_2 (ca. 10 equiv) was added to a dichloromethane solution of **2**. This addition caused the color of the solution to turn from violet to dark orange. After confirmation the oxidation was complete (as inferred from TLC analysis), the insoluble material (presumed to be inorganic salts) was removed by filtration. Since the solubility of **6** is poor once dried, the initial filtrate obtained as the result of this operation was used for all analyses and reactions. ^{1}H NMR (600 MHz, $CDCl_3$, 298 K): $\delta = 21.77$ (brs, 2H; NH), 12.57 (d, $J = 4.8$ Hz, 2H; β-CH), 11.80 (d, $J = 4.8$ Hz, 2H; β-CH), 5.82 (d, $J = 4.6$ Hz, 2H; β-CH), 5.66 (d, $J = 4.6$ Hz, 2H; β-CH), 5.41 (d, $J = 4.6$ Hz, 2H; β-CH), 5.18 ppm (d, $J = 4.6$ Hz, 2H; β-CH); ^{19}F NMR (565 MHz, $CDCl_3$, 298 K): $\delta = -135.7$ (brs, 4F; *o*-F), −138.1 (d, $J = 15.7$ Hz, 4F; *o*-F), −151.6 (t, $J = 21.6$ Hz, 2F; *p*-F), −152.1 (t, $J = 19.1$ Hz, 2F; *p*-F), −160.5 (m, 4F; *m*-F), −162.2 ppm (m, 4F; *m*-F); UV/Vis (CH_2Cl_2): λ_{max} (ε) = 439 (50100), 506 nm (39900 M^{-1} cm^{-1}); HR-ESI-TOF-MS: *m*/*z* (%): calcd for $C_{52}N_6F_{20}H_{14}Na_1$, 1125.0853; found: 1125.2715 (100) [M^++Na].

Bis-zinc complex of [26]rubyrin 7: To a dichloromethane solution of **2** containing a small amount of methanol, was added a mixture of zinc acetate (ca. 10 equiv) and sodium acetate (ca. 10 equiv). Stirring the resulting solution caused the color to change from violet to bright red. The solution was filtered off and all the solvent was removed under reduced pressure to give a crude solid. This solid was redissolved in dichloromethane, layered with hexane and allowed to stand overnight. The solution was filtered and the filtrate was concentrated to dryness to give **7**. ^{1}H NMR (600 MHz, $CDCl_3$, 298 K): $\delta = 10.88$ (brs, 2H; β-CH), 10.37 (brs, 2H; β-CH), 9.57 (d, $J = 4.1$ Hz, 2H; β-CH), 9.52 (brs, 2H; β-CH), 9.34 (d, $J = 4.1$ Hz, 2H; β-CH), 9.04 (brs, 2H; β-CH), −2.87 (s, 3H; CH_3COO), −5.14 (s, 2H; NH), −8.97 ppm (brs, 1H; OH); ^{19}F NMR (565 MHz, $CDCl_3$, 298 K): $\delta = -134.67$ (d, $J = 20.7$ Hz, 2F; *o*-F), −136.96 (d, $J = 20.7$ Hz, 2F; *o*-F), −137.91 (d, $J = 27.3$ Hz, 2F; *o*-F), −138.55 (d, $J = 20.7$ Hz, 2F; *o*-F), −152.25 (t, $J = 20.7$ Hz, 2F; *p*-F), −152.58 (t, $J = 20.7$ Hz, 2F; *p*-F), −161.73 (t, $J = 27.6$ Hz, 2F; *m*-F), −161.98–−162.24 ppm (m, 6F; *m*-F); UV/Vis (CH_2Cl_2): λ_{max} (ε) = 521 (301000), 850 nm (37000 M^{-1} cm^{-1}); MALDI-TOF-MS: *m*/*z* (%): calcd for $C_{52}N_6F_{20}H_{14}Zn_2$: 1229.9544; found: 1229.15 (100) [M^+−OAc−OH].

Bis-zinc complex of [24]rubyrin 8: This complex was prepared in a fashion identical to that used to prepare **7**. ^{1}H NMR (600 MHz, $CDCl_3$, 298 K): $\delta = 6.16$ (d, $J = 4.8$ Hz, 4H; β-CH), 5.22 (d, $J = 4.9$ Hz, 4H; β-CH), 5.15 (s, 4H; β-CH), 4.02 ppm (s, 6H; CH_3COO); ^{19}F NMR (565 MHz, $CDCl_3$, 298 K): $\delta = -138.3$ (d, $J = 20.9$ Hz, 4F; *o*-F), −140.7 (d, $J = 19.9$ Hz, 4F; *o*-F), −152.38 (t, $J = 20.7$ Hz, 4F; *p*-F), −160.9 ppm (m, 8F; *m*-F); UV/Vis (CH_2Cl_2): λ_{max} (ε) = 317 (18000), 423 (48000), 555

(68000), 639 nm (11000 M^{-1} cm^{-1}); HR-ESI-FT-ICR-MS: *m*/*z* (%): calcd for $C_{54}N_6F_{20}H_{15}O_2Zn_2$, 1286.9520; found: 1286.9504 (100) [M^+−OAc].

Acknowledgements

This work was partly supported by Grant-in-Aids (No. 18850003 to S.S. and 19205006 to A.O.) from Japan Society for the Promotion of Science (JSPS) and by the U.S. National Institutes of Health (grant no. GM 588907 to J.L.S.). The authors would like to thank Dr. Elisa Tomat for helpful discussions and suggestions.

[1] a) J. L. Sessler, A. Gebauer, S. J. Weghorn, *The Porphyrin Handbook, Vol. 2* (Eds.: K. M. Kadish, K. M. Smith, R. Guilard), Academic Press, San Diego, **1999**, Chapter 9; b) A. Jasat, D. Dolphin, *Chem. Rev.* **1997**, *97*, 2267–2340; c) T. D. Lash, *Angew. Chem.* **2000**, *112*, 1833–1837; *Angew. Chem. Int. Ed.* **2000**, *39*, 1763–1767; d) H. Furuta, H. Maeda, A. Osuka, *Chem. Commun.* **2002**, 1795–1804; e) J. L. Sessler, D. Seidel, *Angew. Chem.* **2003**, *115*, 5292–5333; *Angew. Chem. Int. Ed.* **2003**, *42*, 5134–5175; f) T. K. Chandrashekar, S. Venkatraman, *Acc. Chem. Res.* **2003**, *36*, 676–691; g) A. Ghosh, *Angew. Chem.* **2004**, *116*, 1952–1965; *Angew. Chem. Int. Ed.* **2004**, *43*, 1918–1931.

[2] a) M. Shionoya, H. Furuta, V. Lynch, A. Harriman, J. L. Sessler, *J. Am. Chem. Soc.* **1992**, *114*, 5714–5722; b) J. L. Sessler, J. M. Davis, *Acc. Chem. Res.* **2001**, *34*, 989–997.

[3] a) R. Charrière, T. A. Jenny, H. Rexhausen, A. Gossauer, *Heterocycles* **1993**, *36*, 1561–1575; b) A. Werner, M. Michels, L. Zander, J. Lex, E. Vogel, *Angew. Chem.* **1999**, *111*, 3866–3870; *Angew. Chem. Int. Ed.* **1999**, *38*, 3650–3653; c) S. J. Weghorn, J. L. Sessler, V. Lynch, T. F. Baumann, J. W. Sibert, *Inorg. Chem.* **1996**, *35*, 1089–1090.

[4] a) S. Shimizu, A, Osuka, *Eur. J. Inorg. Chem.* **2006**, 1319–1335; b) J. L. Sessler, E. Tomat, *Acc. Chem. Res.* **2007**, *40*, 371–379.

[5] a) A. Harriman, B. G. Maiya, T. Murai, G. Hemmi, J. L. Sessler, T. E. Mallouk, *J. Chem. Soc. Chem. Commun.* **1989**, 314–316; b) B. G. Maiya, A. Harriman, J. L. Sessler, G. Hemmi, T. Murai, T. E. Mallouk, *J. Phys. Chem.* **1989**, *93*, 8111–8115.

[6] J. L. Sessler, T. D. Mody, G. W. Hemmi, V. Lynch, S. W. Young, R. A. Miller, *J. Am. Chem. Soc.* **1993**. *115*. 10368–10369.

[7] a) T. K. Ahn, J. H. Kwon, D. Y. Kim, D. W. Cho, D. H. Jeong, S. K. Kim, M. Suzuki, S. Shimizu, A. Osuka, D. Kim, *J. Am. Chem. Soc.* **2005**, *127*, 12856–12861; b) Z. S. Yoon, J. H. Kwon, M.-C. Yoon, M. K. Koh, S. B. Noh, J. L. Sessler, J. T. Lee, D. Seidel, A. Aguilar, S. Shimizu, M. Suzuki, A. Osuka, D. Kim, *J. Am. Chem. Soc.* **2006**, *128*, 14128–14134.

[8] H. Rath, J. Sankar, V. PrabhuRaja, T. K. Chandrashekar, A. Nag, D. Goswami, *J. Am. Chem. Soc.* **2005**, *127*, 11608–11609.

[9] V. J. Bauer, D. L. J. Clive, D. Dolphin, J. B. Paine III, F. L. Harris, M. M. King, J. Loder, S.-W. C. Wang, R. B. Woodward, *J. Am. Chem. Soc.* **1983**, *105*, 6429–6436.

[10] a) A. Gossauer, *Bull. Soc. Chim. Belg.* **1983**, *92*, 793–795; b) A. Gossauer, *Chimia* **1983**, *37*, 341–342; c) A. Gossauer, *Chimia* **1984**, *38*, 45–46.

[11] a) E. Vogel, M. Bröring, J. Fink, D. Rosen, H. Schmickler, J. Lex, K. W. K. Chan, Y.-D. Wu, D. A. Plattner, M. Nendel, K. N. Houk, *Angew. Chem.* **1995**, *107*, 2705–2709; *Angew. Chem. Int. Ed. Engl.* **1995**, *34*, 2511–2514; b) M. Bröring, J. Jendrny, L. Zander, H. Schmickler, J. Lex, Y.-D. Wu, M. Nendel, J. Chen, D. A. Plattner, K. N. Houk, E. Vogel, *Angew. Chem.* **1995**, *107*, 2709–2711; *Angew. Chem. Int. Ed. Engl.* **1995**, *34*, 2515–2517.

[12] a) D. Seidel, V. Lynch, J. L. Sessler, *Angew. Chem.* **2002**, *114*, 1480–1483; *Angew. Chem. Int. Ed.* **2002**, *41*, 1422–1425; b) T. Köhler, D. Seidel, V. Lynch, F. O. Arp, Z. Ou, K. M. Kadish, J. L. Sessler, *J. Am. Chem. Soc.* **2003**, *125*, 6872–6873.

[13] V. G. Anand, S. K. Pushpan, S. Venkatraman, A. Dey, T. K. Chandrashekar, B. S. Joshi, R. Roy, W. Teng, K. Ruhlandt-Senge, *J. Am. Chem. Soc.* **2001**, *123*, 8620–8621.

[14] N. Sprutta, L. Latos-Grażyński, *Chem. Eur. J.* **2001**, *7*, 5099–5112.

[15] a) J.-i. Setsune, Y. Katakami, N. Iizuna, *J. Am. Chem. Soc.* **1999**, *121*, 8957–8958; b) J.-i. Setsune, S. Maeda, *J. Am. Chem. Soc.* **2000**, *122*, 12405–12406.

[16] C.-H. Hung, J.-P. Jong, M.-Y. Ho, G.-H. Lee, S.-M. Peng, *Chem. Eur. J.* **2002**, *8*, 4542–4548.

[17] a) J.-Y. Shin, H. Furuta, K. Yoza, S. Igarashi, A. Osuka, *J. Am. Chem. Soc.* **2001**, *123*, 7190–7191; b) S. Shimizu, J.-Y. Shin, H. Furuta, R. Ismael, A. Osuka, *Angew. Chem.* **2003**, *115*, 82–86; *Angew. Chem. Int. Ed.* **2003**, *42*, 78–82.

[18] a) A. Krivokapic, A. R. Cowley, H. L. Anderson, *J. Org. Chem.* **2003**, *68*, 1089–1096; b) A. Krivokapic, H. L. Anderson, *Org. Biomol. Chem.* **2003**. *1*. 3639–3641.

[19] J. L. Sessler, S. J. Weghorn, V. Lynch, M. R. Johnson, *Angew. Chem.* **1994**, *106*, 1572–1575; *Angew. Chem. Int. Ed. Engl.* **1994**, *33*, 1509–1512.

[20] R. Kumar, R. Misra, T. K. Chandrashekar, *Org. Lett.* **2006**, *8*, 4847–4850.

[21] S. Shimizu, N. Aratani, A. Osuka, *Chem. Eur. J.* **2006**, *12*, 4909–4918.

[22] Rubyrin was first synthesized by Sessler et al., while several core-modified rubyrins have been reported and extensively studied by Chandrashekar and co-workers. a) J. L. Sessler, T. Morishima, V. Lynch, *Angew. Chem.* **1991**, *103*, 1018–1020; *Angew. Chem. Int. Ed. Engl.* **1991**, *30*, 977–980; b) A. Srinivasan, V. M. Reddy, S. J. Narayanan, B. Sridevi, S. K. Pushpan, M. Ravikumar, T. K. Chandrashekar, *Angew. Chem.* **1997**, *109*, 2710–2713; *Angew. Chem. Int. Ed. Engl.* **1997**, *36*, 2598–2601; c) S. J. Narayanan, B. Sridevi, T. K. Chandrashekar, A. Vij, R. Roy, *Angew. Chem.* **1998**, *110*, 3582–3585; *Angew. Chem. Int. Ed.* **1998**, *37*, 3394–3397; d) S. J. Narayanan, B. Sridevi, T. K. Chandrashekar, A. Vij, R. Roy, *J. Am. Chem. Soc.* **1999**, *121*, 9053–9068; e) A. Srinivasan, S. K. Pushpan, M. Ravikumar, T. K. Chandrashekar, R. Roy, *Tetrahedron* **1999**, *55*, 6671–6680; f) S. J. Narayanan, A. Srinivasan, B. Sridevi, T. K. Chandrashekar, M. O. Senge, K. Sugiura, Y. Sakata, *Eur. J. Org. Chem.* **2000**, 2357–2360.

[23] S. Shimizu, R. Taniguchi, A. Osuka, *Angew. Chem.* **2005**, *117*, 2265–2269; *Angew. Chem. Int. Ed.* **2005**, *44*, 2225–2229.

[24] The number in square brackets corresponds to the number of π-electrons in the shortest conjugation pathway, while the core name represents the number of the pyrroles. This nomenclature was first introduced by Franck and Nonn; see: a) T. Wessel, B. Franck, M. Möller, U. Rodewald, M. Läge, *Angew. Chem.* **1993**, *105*, 1201–1203; *Angew. Chem. Int. Ed. Engl.* **1993**, *32*, 1148–1151; b) B. Franck, A. Nonn, *Angew. Chem.* **1995**, *107*, 1941–1957; *Angew. Chem. Int. Ed. Engl.* **1995**, *34*, 1795–1811.

[25] a) S. Mori, J.-Y. Shin, S. Shimizu, F. Ishikawa, H. Furuta, A. Osuka, *Chem. Eur. J.* **2005**, *11*, 2417–2425; b) S. Mori, A. Osuka, *J. Am. Chem. Soc.* **2005**, *127*, 8030–8031; c) S. Mori, K. S. Kim, Z. S. Yoon, S. B. Noh, D. Kim, A. Osuka, *J. Am. Chem. Soc.* **2007**, *129*, 11344–11345.

[26] a) J. L. Sessler, S. J. Weghorn, Y. Hisaeda, V. Lynch, *Chem. Eur. J.* **1995**, *1*, 56–67; b) J. L. Sessler, D. Seidel, A. E. Vivian, V. Lynch, B. L. Scott, D. W. Keogh, *Angew. Chem.* **2001**, *113*, 611–614; *Angew. Chem. Int. Ed.* **2001**, *40*, 591–594; c) P. J. Melfi, S. K. Kim, J. T. Lee, F. Bolze, D. Seidel, V. M. Lynch, J. M. Veauthier, A. J. Gaunt, M. P. Neu, Z. Ou, K. M. Kadish, S. Fukuzumi, K. Ohkubo, J. L. Sessler, *Inorg. Chem.* **2007**, *46*, 5143–5145.

[27] C. Bucher, R. S. Zimmerman, V. Lynch, V. Král, J. L. Sessler, *J. Am. Chem. Soc.* **2001**, *123*, 2099–2100.

[28] a) M. Pohl, H. Schmickler, J. Lex, E. Vogel, *Angew. Chem.* **1991**, *103*, 1737–1741; *Angew. Chem. Int. Ed. Engl.* **1991**, *30*, 1693–1697; b) Y. Yamamoto, A. Yamamoto, S. Furuta, M. Horie, M. Kodama, W. Sato, K. Akiba, S. Tsuzuki, T. Uchimaru, D. Hashizume, F. Iwasaki, *J. Am. Chem. Soc.* **2005**, *127*, 14540–14541; c) J. A. Cissell, T. P. Vaid, A. L. Rheingold, *J. Am. Chem. Soc.* **2005**, *127*, 12212–12213;

d) J. A. Cissell, T. P. Vaid, G. P. A. Yap, *Org. Lett.* **2006**, *8*, 2401–2404; e) J. A. Cissell, T. P. Vaid, G. P. A. Yap, *J. Am. Chem. Soc.* **2007**, *129*, 7841–7847.

[29] Gaussian 03, Revision B 05, M. J. Frisch, G. W. Trucks, H. B. Schlegel, G. E. Scuseria, M. A. Robb, J. R. Cheeseman, J. A. Montgomery, Jr., T. Vreven, K. N. Kudin, J. C. Burant, J. M. Millam, S. S. Iyengar, J. Tomasi, V. Barone, B. Mennucci, M. Cossi, G. Scalmani, N. Rega, G. A. Petersson, H. Nakatsuji, M. Hada, M. Ehara, K. Toyota, R. Fukuda, J. Hasegawa, M. Ishida, T. Nakajima, Y. Honda, O. Kitao, H. Nakai, M. Klene, X. Li, J. E. Knox, H. P. Hratchian, J. B. Cross, V. Bakken, C. Adamo, J. Jaramillo, R. Gomperts, R. E. Stratmann, O. Yazyev, A. J. Austin, R. Cammi, C. Pomelli, J. W. Ochterski, P. Y. Ayala, K. Morokuma, G. A. Voth, P. Salvador, J. J. Dannenberg, V. G. Zakrzewski, S. Dapprich, A. D. Daniels, M. C. Strain, O. Farkas, D. K. Malick, A. D. Rabuck, K. Raghavachari, J. B. Foresman, J. V. Ortiz, Q. Cui, A. G. Baboul, S. Clifford, J. Cioslowski, B. B. Stefanov, G. Liu, A. Liashenko, P. Piskorz, I. Komaromi, R. L. Martin, D. J. Fox, T. Keith, M. A. Al-Laham, C. Y. Peng, A. Nanayakkara, M. Challacombe, P. M. W. Gill, B. Johnson, W. Chen, M. W. Wong, C. Gonzalez, J. A. Pople, Gaussian, Inc., Wallingford CT, **2003**.

[30] a) A. D. Becke, *Phys. Rev. A* **1988**, *38*, 3098–3100; b) C. Lee, W. Yang, R. G. Parr, *Phys. Rev. B* **1988**, *37*, 785–789.

[31] a) P. von R. Schleyer, C. Maerker, A. Dransfeld, H. Jiao, N. J. van E. Hommes, *J. Am. Chem. Soc.* **1996**, *118*, 6317–6318; b) P. von R. Schleyer, H. Jiao, N. J. van E. Hommes, V. G. Malkin, O. L. Malkina, *J. Am. Chem. Soc.* **1997**, *119*, 12669–12670.

[32] A. Altomare, M. C. Burla, M. Camalli, G. L. Cascarano, C. Giacovazzo, A. Guagliardi, A. G. G. Moliterni, G. Polidori, R. Spagna, *J. Appl. Crystallogr.* **1999**, *32*, 115–119.

[33] G. M. Sheldrick, SHELXS-97 and SHELXL-97, Program for the Solution and Refinement of Crystal Structures, University of Göttingen, Göttingen (Germany), **1997**.

[34] a) P. V. Sluis, A. L. Spek, *Acta Crystallogr. Sect. A* **1990**, *46*, 194–201; b) A. L. Spek, *Acta Crystallogr. Sect. A* **1990**, *46*, c34.

Received: December 4, 2007
Published online: February 12, 2008

